

# Journal of Materials Chemistry A

Accepted Manuscript



This is an *Accepted Manuscript*, which has been through the Royal Society of Chemistry peer review process and has been accepted for publication.

*Accepted Manuscripts* are published online shortly after acceptance, before technical editing, formatting and proof reading. Using this free service, authors can make their results available to the community, in citable form, before we publish the edited article. We will replace this *Accepted Manuscript* with the edited and formatted *Advance Article* as soon as it is available.

You can find more information about *Accepted Manuscripts* in the [Information for Authors](#).

Please note that technical editing may introduce minor changes to the text and/or graphics, which may alter content. The journal's standard [Terms & Conditions](#) and the [Ethical guidelines](#) still apply. In no event shall the Royal Society of Chemistry be held responsible for any errors or omissions in this *Accepted Manuscript* or any consequences arising from the use of any information it contains.

Cite this: DOI: 10.1039/c0xx00000x

ARTICLE TYPE

www.rsc.org/xxxxxx

## UF membrane with highly improved flux by hydrophilic network between graphene oxide and brominated poly(2,6-dimethyl-1,4-phenylene oxide)

Lijia Yang, Beibei Tang\* and Peiyi Wu\*

Received (in XXX, XXX) Xth XXXXXXXXX 20XX, Accepted Xth XXXXXXXXX 20XX

DOI: 10.1039/b000000x

In this work, graphene oxide (GO) was first functionalized with branched polyethyleneimine (PEI). The obtained PEI-GO was incorporated into brominated poly(2,6-dimethyl-1,4-phenylene oxide) (BPPO) matrix by covalently bonding interaction to form a cross-linking network. Then, a novel ultrafiltration (UF) membrane was prepared via casting and phase inversion method. The PEI-GO/BPPO membrane showed highly improved water flux which was almost 6 times higher than that of the pristine BPPO membrane and 2.5 times higher than that of the GO/BPPO membrane. While the rejection of PEI-GO/BPPO membrane still maintained at a high level. The improvement of membrane performance could be attributed to the special property of PEI-GO and the interactions between PEI-GO and BPPO matrix. Firstly, a cross-linking network of PEI-GO/BPPO membrane was formed due to the reaction between PEI-GO and BPPO matrix to provide passageways for water rapidly passing through. Secondly, the high hydrophilicity of PEI-GO could accelerate the exchange rate between solvent and non-solvent, resulting in a rougher and more hydrophilic surface, and higher porosity and more porous structure. Thirdly, the good dispersion and compatibility of PEI-GO promoted the formation of a uniform structure with less defects. Proper molecular weight of PEI was very important for the modification of GO, subsequently resulting in an overall enhancement in membrane performance. Anti-fouling experiments and stability test of membranes were also conducted. All these results were confirmed by various characterizations, such as SEM, TEM, AFM and etc.

### 1 Introduction

Membrane separation has been proved to be an effective and efficient way to regenerate clean water due to its low cost, simple operation, environmental-friendly adaptability and etc.<sup>1,2</sup> Especially, ultrafiltration (UF) membrane attracts enormous attentions in the water treatment because of its excellent performance at the removal of particles, proteins and so on<sup>3-5</sup>. Generally, it is of necessity in practical separation operations that a UF membrane possesses high permeability and suitable selectivity. Additionally, anti-fouling property of membrane also plays an important role in the operation and maintenance costs, membrane performance stability and membrane lifetime. Hydrophilic modification of UF membrane is a common approach to improve the membrane permeability and anti-fouling property, because the hydrophilicity always facilitates reduction in the flow resistance and enhancement of permeation and prevents irreversible adhesion of contaminations<sup>6-9</sup>. To achieve a high hydrophilic UF membrane, incorporating inorganic materials, such as silica<sup>10-13</sup>, TiO<sub>2</sub><sup>6,14</sup> and ZrO<sub>2</sub><sup>15</sup>, into polymer matrix has been widely studied. It has been proved that the

obtained organic-inorganic hybrid membranes exhibit higher hydrophilicity, permeability and other improved performance.

Recently, using graphene oxide (GO) as a membrane improver becomes a hotspot due to GO's unique properties, such as multiple oxygen containing functionalities, good mechanical stability and water permeation and so on<sup>16,17</sup>. Yang et al.<sup>18-20</sup> prepared a novel GO/PES mixed matrix membrane via phase inversion method and found that the membrane modified with GO demonstrated increased hydrophilicity and water flux. Fang et al.<sup>7,21,22</sup> studied the role of GO in the membrane structure during the phase inversion. The porosity and mean pore size of membrane increased and thus an enhanced permeability was obtained when GO was incorporated into PVDF matrix. However, the dispersion and compatibility of inorganic component in polymer matrix is still a challenge for excellent membrane performance. For example, GO easily stacks together, forming nonselective voids in the membrane and resulting in a deterioration of selectivity<sup>19</sup>.

It seems that grafting polymers can effectively increase the dispersion and compatibility between the inorganic fillers and organic matrix<sup>12,23-25</sup>. For example, Kim et al.<sup>26,27</sup> grafted poly(1-

vinylpyrrolidone) (PVP) on SiO<sub>2</sub> to improve SiO<sub>2</sub>'s dispersion in PVDF. Madaeni et al.<sup>23</sup> reported the modification of PVDF by grafting polymerization of acrylic acid functionalized TiO<sub>2</sub> and prepared an anti-fouling membrane with better dispersion of TiO<sub>2</sub>. Among these polymer media, polyethyleneimine (PEI) is widely employed because it can endow the membrane with extra performance due to the existence of a large number of amine groups on its molecule. For instance, Mauter et al.<sup>24,25</sup> utilized PEI to encapsulate Ag nanoparticle and then to react with the oxygen plasma modified PSf membrane. The resulted membrane exhibited a huge potential in antimicrobial applications. Zhang et al.<sup>28</sup> prepared the PEI-GO/PES composite membrane by blending PEI functionalized GO with PES. The composite membrane showed preferable anti-fouling ability, good tensile strength and Young's modulus. However, the water permeation of the PEI-GO/PES membrane decreased with PEI-GO adding. It was an unexpected result. Therefore, only modifying inorganic particle by polymer medium to increase the compatibility between the inorganic improver and organic matrix may be not enough. Design and construction interactions, especially, chemical bonds, between two components perhaps will grant the membrane surprisingly good performance.

In this paper, GO was first functionalized with branched PEI and the synthesized PEI-GO was covalently bonded with brominated poly (2,6-dimethyl-1,4-phenylene oxide) (BPPO) via nucleophilic reaction between PEI and benzyl bromide of BPPO. Then, a cross-linking network of PEI-GO/BPPO membrane was formed to provide passageways for water rapidly passing through. The prepared PEI-GO/BPPO membrane exhibited a highly improved permeation rate compared with the pristine BPPO and GO/BPPO membrane yet a slight decrease in rejection. The influences on the membrane performance and morphology of PEI's molecule weight and PEI-GO's weight fraction were investigated as well. All the results were supported in terms of FTIR, crosslinking degree, pure water flux, rejection, SEM, AFM and et al.

## 2 Experimental section

### 2.1 Materials

Expandable graphite powders were provided by Yingtai Co. (China). Branched polyethyleneimine (Aladdin, Mw= 1,800 and 10,000). The brominated PPO (BPPO) was obtained by the bromination of PPO as described in our previous paper<sup>10,29,30</sup>. N-methyl-2-pyrrolidone (NMP) and bromine, were all of analytical grade. BSA (Mw= 68,000) was used as a probe molecule for rejection tests and supplied by Sinopharm Chemical Reagent Co., Ltd. Unless otherwise stated, all the other reagents were purchased from commercial suppliers and used as received.

### 2.2 Synthesis of PEI-GO

#### 2.2.1 Preparation of GO

GO was synthesized by modified Hummers method as reported in our previous works<sup>31,32</sup>.

#### 2.2.2. Preparation of PEI-GO

PEI-GO was synthesized according to the "one-spot" method reported by Liu et al.<sup>33</sup> with a modification. Briefly, 500 mg of the resultant GO dispersion and 2,000 mg of PEI (Mw=1,800 and 10,000) were mixed in a beaker under vigorous stirring. A further

reaction occurred with continuous stirring at 80 °C for 2 h. The PEI-GO from different Mw PEI was purified by repeat centrifugation (10,000 rpm) with DI water. At last, the PEI-GO was dispersed in NMP at an appropriate concentration.

### 2.3. Membrane preparation

The UF membranes were prepared via phase inversion method as described in our previous papers<sup>10,29,34,35</sup>. Briefly, after BPPO was dissolved in NMP, a yellow transparent solution formed. Then PEI-GO/NMP was added into the BPPO/NMP solution according to the weight fraction of PEI-GO at room temperature and the mixture stirred overnight. The resulted casting solution became dark and its viscosity increased a little but without gelation. Finally, this solution was cast onto a clean glass after ultrasound stirring and bubble removal. Subsequently, the glass was immersed into DI water at a temperature of 30 °C for at least 24 h. At last, the membranes were washed with DI water repeatedly and stored in a wet environment. For comparison, BPPO membrane with GO loading of 0.6% (w/w) and pristine BPPO membrane were prepared using the same method. Unless otherwise stated, the molecular weight of PEI is 1,800. BPPO based composite membranes containing 0.2, 0.4, 0.6, 0.8 and 1.0% (w/w) PEI-GO with respect to polymer are denoted as PEI-GO/BPPO-0.2, PEI-GO/BPPO-0.4, PEI-GO/BPPO-0.6, PEI-GO/BPPO-0.8 and PEI-GO/BPPO-1.0, and containing 0.6% (w/w) GO as GO/BPPO.

### 2.4. Characterization

#### 2.4.1. Characterizations of PEI-GO

Fourier transform infrared (FT-IR) spectra were recorded on Nicolet Nexus 470 with a resolution of 4 cm<sup>-1</sup> and 32 scans. The TGA analyses were performed under N<sub>2</sub> atmosphere with a Perkin Elmer Thermal Analyzer at a heating rate of 20 °C·min<sup>-1</sup> from 100 °C to 600 °C. The grafting degree of PEI was calculated from Elemental Analysis (VARIO EL3, ELEMEN TAR, German). X-ray diffraction (XRD, PANalytical X'pert diffractometer with Cu K $\alpha$  radiation) and Ultraviolet-visible spectrophotometer (Lambda 35, PerkinElmer, USA) was utilized to confirm the synthesis of PEI-GO. The Raman spectra were collected on a Renishaw inVia Reflex micro-Raman spectrometer with 633 nm laser excitation. The Atomic force microscopic (AFM) images were obtained using a Multimode 8 in the tapping mode.

#### 2.4.2. Characterizations of membranes

The FT-IR spectra were recorded on a Nicolet Nexus 470 spectrometer with a resolution of 4 cm<sup>-1</sup> and 128 scans with the ATR accessory. The TGA analyses were performed under N<sub>2</sub> atmosphere with a Perkin Elmer Thermal Analyzer at a heating rate of 20 °C·min<sup>-1</sup>.

##### 2.4.2.1. Membrane morphology

Both the surface and the cross-sectional morphologies of all membranes were observed with a SEM (XL 30 ESEM-TMP PHILIP). All the samples were coated with gold before the SEM observation. The cross-sectional TEM (transmission electron microscopy) image of the PEI-GO/BPPO-0.6 composite membrane was recorded on a JEOL JEM 2100 TEM instrument to investigate the dispersion of PEI-GO in the BPPO matrix. The Atomic force microscopic (AFM) images were obtained using a Multimode 8 in the tapping mode.

#### 2.4.2.2. Mechanical properties

Tensile strength and tensile modulus were measured on Instron 5565 mechanical testing instrument (speed: 60% min<sup>-1</sup>, 50-60% RH) mounted with a 500 N load at room temperature.

#### 2.4.2.3. Streaming potential

The streaming potential (SP) measurement was taken as reported in our previous works.<sup>34</sup>

#### 2.4.2.4. Flux and separation experiments

The measurements of pure water flux and protein rejection were performed using a cross-flow membrane module as described in our previous reports<sup>10,29,34</sup>, and it had an effective area of 2.6×10<sup>-3</sup> m<sup>2</sup> for every membrane. Both the pure water flux and rejection test were conducted at an operation pressure of 0.2 MPa. The water flux ( $F$ ) was calculated in Eq. (1):

$$F = \frac{V}{A \times t} \quad (1)$$

Where  $V$  is the total volume of permeated pure water,  $A$  is the membrane area, in this case, 2.6×10<sup>-3</sup> m<sup>2</sup>, and  $t$  is the operation time. DI water was used for this measurement. The rejection was measured using 0.5 g/L BSA solution at pH 4.7. The concentrations of the permeation and feed solutions were determined by UV measurement at 280 nm. The rejection,  $R$ , was calculated in Eq. (2)

$$R = 1 - \frac{C_p}{C_f} \quad (2)$$

Where  $C_p$  and  $C_f$  are concentrations of the permeation and feed solutions, respectively.

#### 2.4.2.5. Water uptake

The water uptake (WU) was used to investigate the water retention capability of each UF membrane. The detailed description of experiment can be achieved in our previous papers.<sup>32,36</sup>

#### 2.4.2.6. Determination of coagulation value

The measurement was taken as follows. Non-solvent (DI water) was slowly added into a 50 g casting solution containing 0.5 g BPPO, while stirred intensively until the first appearance of turbidity (the coagulation of the polymeric solution) was visually observed and did not re-dissolve at temperature of 25 °C in 24 h. The coagulation value was then calculated as the ratio of non-solvent (g) to polymer solution plus non-solvent (g)<sup>35</sup>.

#### 2.4.2.7. Crosslinking degree

The crosslinking degree measurement was conducted by immersing dried membrane samples into the solvent (NMP) for 24 h at 30 °C. Then, the samples were washed with deionized water repeatedly and dried in vacuum. The crosslinking degree ( $D$ ) was calculated in Eq. (3):

$$D = \frac{W_2}{W_1} \quad (3)$$

$W_1$  and  $W_2$  are weights of the original and treated membrane samples, respectively.

#### 2.4.2.8. Anti-fouling performance

For anti-fouling investigations, the operating pressure was 0.2 MPa for the whole process. The experiments were performed as

shown in our previous reports<sup>37</sup>. After the pure water permeability  $J_0$  was measured, the flux for BSA (0.5 g/L, pH=4) solution  $J_p$  was measured. The filtration of the BSA solution kept for 1h and then the membrane was washed with DI water for 2 h, the water flux  $J_R$  of the cleaned membranes was measured again. The flux recovery ratio ( $FRR$ ), Reversible fouling resistance ( $R_r$ ) and Irreversible fouling resistance ( $R_{ir}$ ) were calculated as follows:

$$FRR = \frac{J_R}{J_0} \quad (4)$$

$$R_r = \frac{J_R - J_p}{J_0} \quad (5)$$

$$R_{ir} = \frac{J_0 - J_R}{J_0} \quad (6)$$

A short-term stability test was performed on the PEI-GO/BPPO composite membrane using the same method as anti-fouling performance measurement. The process lasted at least 5 days.

## 3 Results and Discussion

### 3.1 Characterization of PEI-GO

As shown in Fig. 1A, GO has a typical peak at 1733 cm<sup>-1</sup> ascribed to C=O stretching vibration. While the FTIR spectrum of PEI-GO shows not only the peak at 2940 and 2830 cm<sup>-1</sup> corresponding to the methylene groups of PEI but also new peaks at 1645 and 1570 cm<sup>-1</sup> attributed to the O=C-NH stretching vibration<sup>38</sup>. It means that the carboxy groups of GO react with the amine groups of PEI to form amide<sup>39,40</sup>. In the UV-vis spectra of GO and PEI-GO dispersion as shown in Fig. 1B, the absorption peaks appear at 234 and 263 nm, respectively. This peak shift in PEI-GO is caused by the restoration of  $\pi$ -electron conjugation within graphene sheets<sup>33</sup> due to the formation of chemical bonds between GO and PEI. TGA analyses of GO and PEI-GO are shown in Fig. 1C. For GO, a sharp loss around 220 °C attributes to the pyrolysis of oxygen-containing groups from the surface of GO sheets<sup>16</sup>. While in the case of PEI-GO, a gradual mass loss in the range of 260–500 °C mainly corresponding to the pyrolysis of the covalently bonded PEI molecules<sup>41</sup> is observed. According to element analysis, PEI-GO contains approximately 41.9% (w/w) covalently bonded PEI. In the XRD pattern (Fig. 1D) of GO, a sharp and intensive peak at  $2\theta = 10.6^\circ$  is corresponding to the interlayer spacing of 0.832 nm<sup>42</sup>. While for PEI-GO, the long chain of PEI can intercalate between the sheets and expand the intersheet gallery of GO because of the covalent bonding interaction between PEI and GO sheets<sup>41</sup>. As a result, a strong peak at  $2\theta = 5.40^\circ$  shows up in the XRD pattern of PEI-GO, indicating an increased spacing of 1.60 nm. Besides, it is noted that a diffraction peak at  $2\theta = 21.9^\circ$  occurs. Because PEI may not fill the space between GO sheets completely, the loss of oxygen containing groups during reaction between PEI and GO induces the interlayer spacing to decrease to 0.403 nm<sup>43,44</sup>. In the Raman spectrum of GO as shown in Fig. 1E, two characteristic peaks appear at 1336 cm<sup>-1</sup> (D band) and 1594 cm<sup>-1</sup> (G band), respectively. While in the PEI-GO's, G band shifts to 1584 cm<sup>-1</sup>

and the  $I_D/I_G$  ratio substantially increases. The results are derived from the nucleophilic reaction between amine groups of PEI and the epoxy or carboxyl groups of GO, thus leading to the loss of oxygen containing groups and the formation of covalent bonds. Moreover, AFM measurement reveals that the thickness of PEI-

GO sheet increases to 2-3 nm (Fig. 1F and 1G) because of PEI binding on GO sheet<sup>45</sup>. All the characterization results show that the PEI-GO is synthesized successfully.

10

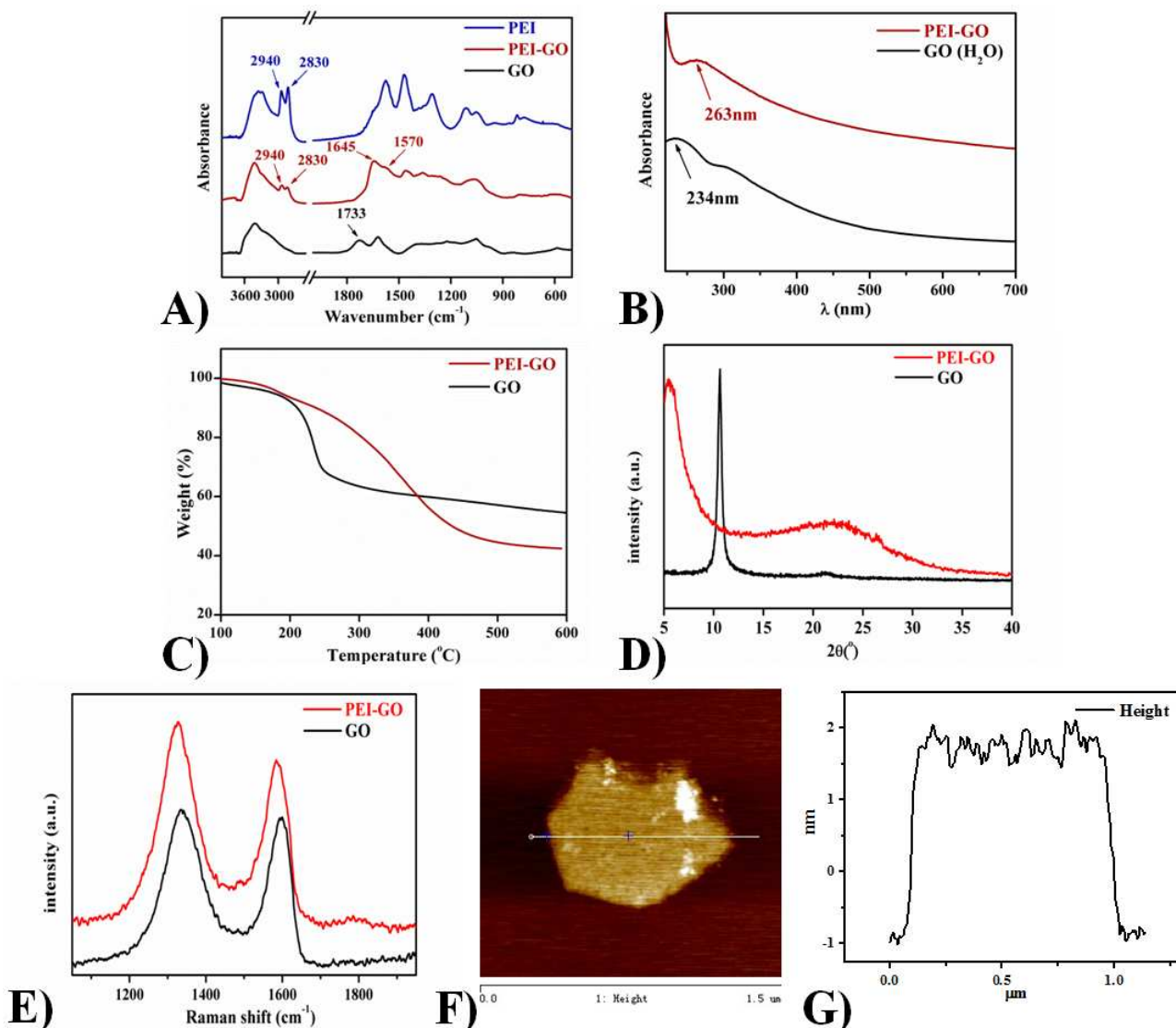


**Fig.1** (A) FT-IR spectra of GO, PEI and PEI-GO, (B) UV-vis spectra analyses of GO and PEI-GO, both dispersed in water aqueous, (C) TGA, (D) XRD patterns and (E) Raman spectra of GO and PEI-GO and (F, G) AFM image of PEI-GO with height profile.

### 3.2 Characterization of PEI-GO /BPPO composite membranes

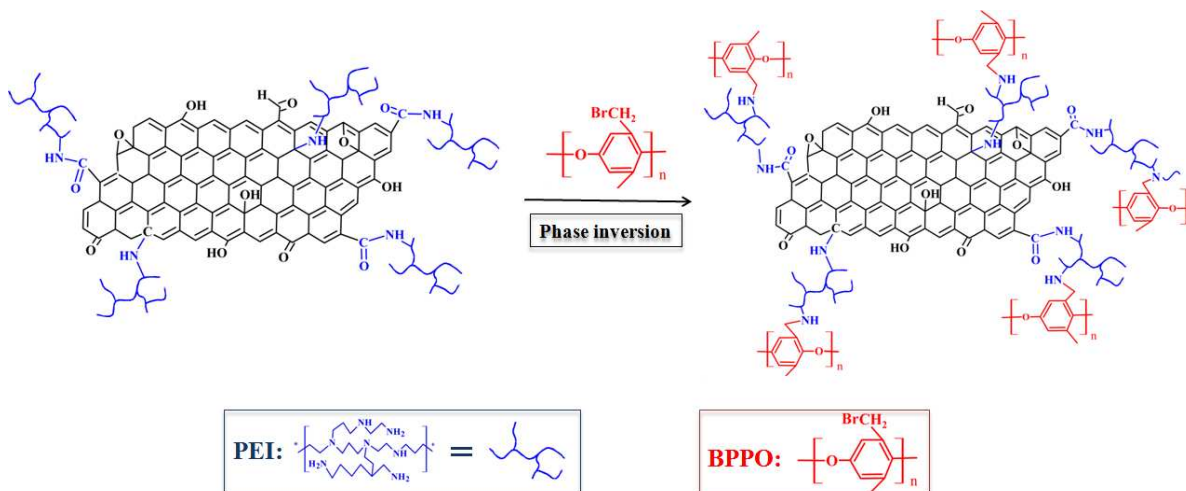
When the PEI-GO is added into the BPPO solution, nucleophilic substitution reaction between PEI-GO and BPPO occurs, consequently, forming a cross-linking network structure as shown in Scheme 1.

In this section, PEI-GO/BPPO refers to the PEI-GO/BPPO-0.6 composite membrane. The FTIR spectra of BPPO membrane and PEI-GO/BPPO composite membrane are shown in Fig. 2A. In the spectrum of PEI-GO/BPPO membrane, the band at 1645

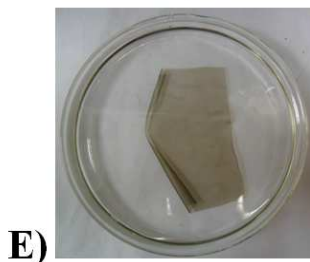
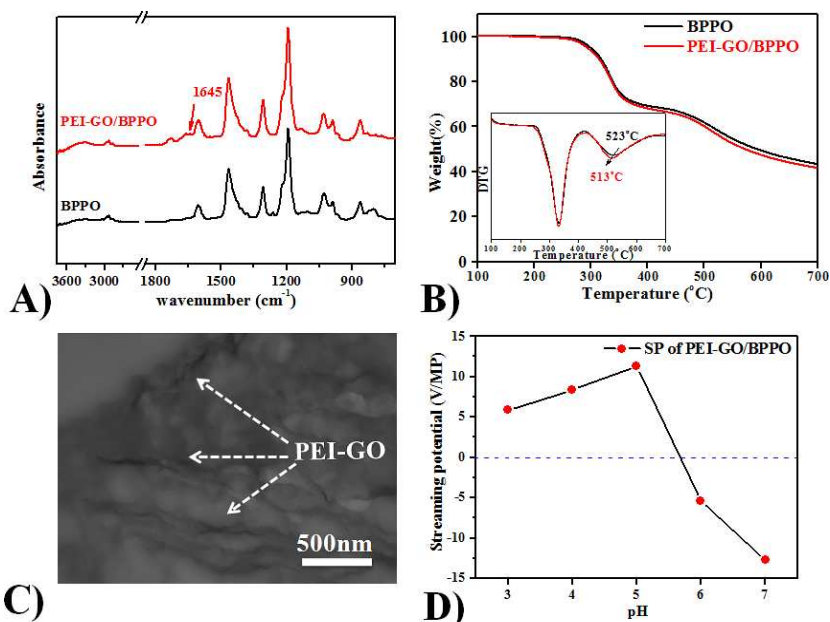
$\text{cm}^{-1}$  is assigned to the C=O stretching vibration of PEI-GO. Besides, the intensity of the peak around  $3400 \text{ cm}^{-1}$  ascribed to N-H stretching vibration is decreased compared with that in the spectrum of PEI-GO sheet. It is derived from the reactions between amine groups of PEI-GO and BPPO. TGA analyses of BPPO membrane and PEI-GO/BPPO composite membrane are represented in Fig. 2B. The temperature corresponding to the highest decomposition rate of PEI-GO/BPPO membrane (513 °C) is slightly lower than that of the BPPO membrane (523 °C). It illustrates that the addition of PEI-GO accelerates the pyrolysis of BPPO matrix. This can be attributed to the covalently bonding

interactions between PEI-GO and BPPO. As discussed in Fig. 1C, the PEI-GO loses weight severely in the range of 260-500 °C and BPPO polymer chains become more flexible with the decoration of PEI-GO sheets, thus leading to a decrease in the thermal stability of PEI-GO/BPPO composite membrane. The dispersion of the PEI-GO in the membrane can be observed by TEM image shown in Fig. 2C. The PEI-GO sheets disperse well in BPPO matrix without apparent agglomerations. Fig. 2D presents the streaming potential (SP) of PEI-GO/BPPO membrane at different pH. It implies that the PEI-GO/BPPO membrane is amphoteric,

deriving from the existence of amine groups of PEI and residual -COOH groups of GO in the membrane structure. Furthermore, the etching experiment shown in Fig. 2E demonstrates that the PEI-GO/BPPO membrane still remains its complete shape after being immersed in NMP for 24h. It suggests that a hydrophilic cross-linking network structure of BPPO and PEI-GO is formed during the membrane formation. Besides, it implicitly confirms the good dispersion and compatibility of PEI-GO in BPPO matrix.



Scheme 1 Schematic of the reaction between PEI-GO and BPPO.



20

**Fig. 2** (A) FT-IR spectra, (B) TGA/DTG measurements of BPPO membrane and PEI-GO/BPPO membrane, (C) TEM picture, (D) streaming potential of PEI-GO/BPPO membrane and (E) digital figure of PEI-GO/BPPO membrane in NMP after etched for 24h. The content of PEI-GO in the composite membrane is 0.6% (w/w).

The membrane performances in terms of pure water flux and rejection of BPPO membrane, GO/BPPO composite membrane and PEI-GO/BPPO composite membrane are compared and the results are presented in Fig. 3A. Both composite membranes incorporated inorganic particles show higher permeate fluxes compared with the pristine BPPO membrane. Especially, the permeate flux of PEI-GO/BPPO membrane is 1065 L·m<sup>-2</sup>·h<sup>-1</sup>, nearly 6 times higher than that of BPPO membrane (156 L·m<sup>-2</sup>·h<sup>-1</sup>) and 2.5 times higher than that of GO/BPPO membrane (331 L·m<sup>-2</sup>·h<sup>-1</sup>) at the same operation pressure. It has been reported that the oxidized regions of GO, strongly interacting with intercalating water, are likely to contribute to the composite

membrane's water permeation<sup>46</sup>. Additionally, with the help of PEI in the present study, a hydrophilic cross-linking network between GO and BPPO is formed, which can provide the passageways for water rapidly passing through, thereby, resulting in the enhancement of water permeation. The water uptake (WU) measurements are as shown in Fig. 3B. The PEI-GO/BPPO composite membrane exhibits the highest water retention capability, which is consistent with the results of the water permeation test. Besides, the good dispersion and compatibility of PEI-GO in/with BPPO benefit to the membrane's hydrophilicity and facilitate the water passages as well.

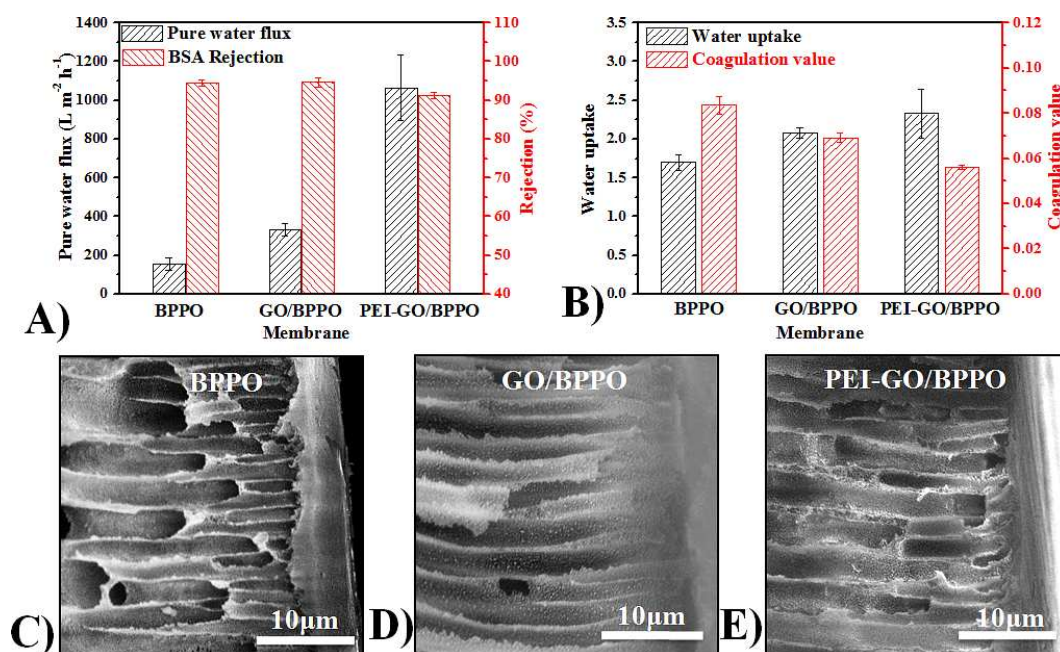


**Fig. 3** (A) Pure water flux and rejection to BSA (0.5 g/L, pH=4.7) test at 0.2 MPa operating pressure, (B) water uptake and coagulation value, (C, D and E) cross-sectional SEM figures of BPPO, GO/BPPO, PEI-GO/BPPO membranes, respectively. The content of PEI-GO in the composite membrane is 0.6% (w/w).

Furthermore, the high hydrophilicity of PEI-GO incorporated into polymer matrix can accelerate the exchange rate between solvent and non-solvent, resulting in rougher and more hydrophilic surface and more porous structure. Therefore, the thermal stabilities of three casting solutions (BPPO, GO/BPPO, and PEI-GO/BPPO) were investigated by coagulation value. The higher the coagulation value of the casting solution is, the better the thermodynamic stability is<sup>30,35,47</sup>. In other words, the lower the coagulation value becomes, the quicker the phase inversion turns. Fig. 3B illustrates that the coagulation value of PEI-GO/BPPO casting solution is the lowest in the three studied casting solutions, which means the phase inversion speed of PEI-GO/BPPO casting solution is the fastest, thus easily forming higher porosity and more porous structure. The pore structures of membranes are displayed in Fig. 3 (C, D and E). The PEI-GO/BPPO membrane displays a porous and a little bigger finger-like structure. It can also be proved by the result of rejection. In Fig. 3A, the rejections to BSA of three membranes exhibit slight

differences, which are 94%, 94%, and 91% respectively for BPPO, GO/BPPO and PEI-GO/BPPO membrane. It should be noted that the pH of feed solution was adjusted to 4.7 which is the isoelectric point of BSA. Therefore, the rejection mechanism is mainly dependent on the sieving effect. The decrease in rejection of the PEI-GO/BPPO membrane is derived from the more porous structure. However, the cross-linking network structure formed by PEI-GO reacting with BPPO as shown in Scheme 1, prevents further loss in rejection of PEI-GO/BPPO membrane. Moreover, we speculate the roughness of membrane surface is another important factor to achieve high flux. Rough surface commonly leads to an increase in efficient filtration area, thus enhancing the membrane permeation directly<sup>48,49</sup>. The roughness of the membrane surface is determined by AFM as shown in Fig. 4 (A, B and C) and is quantified in Table 2. The order of roughness in terms of Rq (root mean square height) is: BPPO membrane < GO/BPPO composite membrane < PEI-GO/BPPO composite membrane, which is consistent with the morphologies observed

by SEM images (Fig. 4C, D and E). Therefore, the incorporation of PEI-GO into BPPO matrix promotes formation of hydrophilic cross-linking network and increases the hydrophilicity, pore size,

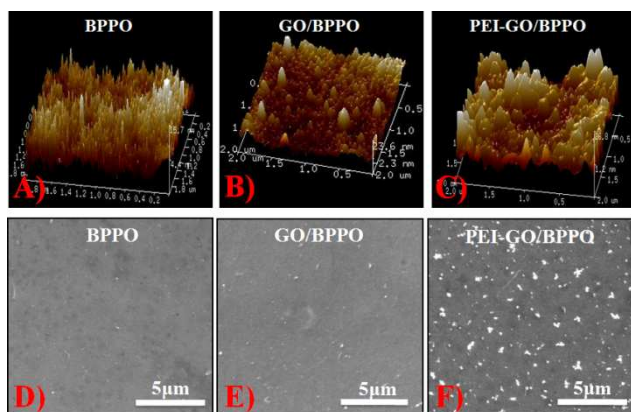


**Fig. 4** AFM three-dimensional surface images of (A) BPPO membrane, (B) GO/BPPO composite membrane, (C) PEI-GO/BPPO composite membrane, SEM images of surface of (D) BPPO membrane, (E) GO/BPPO composite membrane and (F) PEI-GO/BPPO composite membrane. The content of PEI-GO in the composite membrane is 0.6% (w/w).

**Table 2** Surface roughness values of BPPO, GO/BPPO and PEI-GO/BPPO Membranes

Membrane	Rq (nm)	Ra (nm)
BPPO	2.9	2.3
GO/BPPO	6.5	5.0
PEI-GO/BPPO	9.3	7.4

The mechanical properties of BPPO, GO/BPPO, PEI-GO/BPPO membranes show in Table 1.

**Table 1** Tensile strength and tensile modulus of BPPO, GO/BPPO, PEI-GO/BPPO membranes

Membrane	Tensile strength (MPa)	Tensile modulus (MPa)
BPPO	5.78±0.82	151±10
GO/BPPO	6.42±0.51	155±11
PEI-GO/BPPO	7.52±0.16	165±14

The change of tensile modulus is not obvious, but the tensile strength increases when inorganic component being added. Especially, the PEI-GO/BPPO composite membrane exhibits 30% higher tensile strength than the pristine BPPO membrane. It reveals that the covalently bonding interactions between PEI-GO and BPPO and the cross-linking network can effectively enhance the composite membrane's mechanical properties.

Conclusively, the addition of PEI-GO into BPPO not only facilitates the formation of cross-linking network structure between PEI-GO and BPPO matrix, endowing the composite membrane with better mechanical properties, but also accelerates the phase inversion because of more favourable chemical affinity between water and casting solution. What's more, incorporation of PEI-GO invites more porous and higher porosity structure and makes the composite membrane surface rougher, thereby leading to a highly improved water flux with a slight decrease of rejection.

### 3.3 Effect of different molecular weight of PEI on the membrane performance and morphologies

In this section, we try to investigate the effect of molecular

porosity and roughness of the membrane surface, which can contribute to the improvement of water permeation<sup>50</sup>.

weight (Mw) of PEI on the modification of GO and the consequent PEI-GO/BPPO membrane. PEI with Mw of 10,000 was chosen to compare with PEI with Mw of 1,800 and PEI-GO sheets were prepared via the same modified "one-spot" method. Fig. 5A shows the TGA measurement of PEI (10,000)-GO. The weight loss at 260-500 °C is mainly assigned to the pyrolysis of the covalently bonded PEI, which is similar to PEI (1,800)-GO. The mass loss from 150 to 220 °C is mainly attributed to the removal of residual oxygen-containing groups<sup>16</sup>. Accordingly, the covalently bonded PEI in PEI-GO can be calculated based on the element analysis results, which are approximately 41.9 and 25.4% (w/w) respectively for PEI's Mw 1,800 and 10,000. We speculate that higher molecular weight of PEI is unfavourable to modify GO because its branched chains are most likely to extend significantly away from the GO surface and easily interact with other negatively charged GO<sup>51</sup>, thus occurring aggregations<sup>52</sup> and leaving more oxygen containing groups on GO.

Fig. 5B shows the pure water fluxes and rejection tests of PEI (1,800)-GO/BPPO and PEI (10,000)-GO/BPPO membranes whose contents of PEI-GO are both 0.6% (w/w). The water permeation rate of PEI (1,800)-GO/BPPO membrane is much higher than that of PEI (10,000)-GO/BPPO membrane as expected. As discussed in Section 3.2, cross-linking network, hydrophilicity, pore structure, porosity and surface roughness play important roles in the water permeation. Fig. 5C shows the water uptakes of two membranes. The PEI (1,800)-GO/BPPO membrane shows higher WU value than that of PEI (10,000)-GO/BPPO membrane. Fig. 6 shows the cross-sectional, surface SEM and surface AFM images of membranes with different Mw of PEI. The membrane with PEI's Mw of 1,800 has bigger pore size and higher porosity as well as rougher surface. The surface roughness of the PEI (1,800)-GO/BPPO membrane in terms of Rq is almost 2 times higher than that of the PEI (10,000)-GO/BPPO membrane. The factors mentioned above together contribute to the high permeability of PEI (1,800)-GO/BPPO membrane. Then, why the Mw of PEI has such a significant effect on the membrane performance? As demonstrated in Scheme 1, PEI-GO works as joints and crosslinkages between the BPPO chains due to nucleophilic substitution reaction between amine groups of PEI and benzyl bromide groups of BPPO, which promotes the dispersion and compatibility of inorganic particles in polymer matrix as well as facilitates the formation of hydrophilic cross-linking network. Therefore, the amount of PEI decorated on GO is a crucial factor, which decides the interaction degree between PEI-GO and BPPO, and hydrophilicity of PEI-GO. According to the PEI grafting degree, the amount of covalently bonded PEI of PEI (1,800)-GO is much higher than that of PEI (10,000)-GO. It means that PEI of Mw 1,800 modifies GO better and provides more amine groups for a further modification. It can also be certificated by the result of cross-linking degree of membranes (Fig. 5 C). The membrane prepared from PEI's Mw of 1800 possesses a higher cross-linking degree, almost two times as that of the PEI (10,000)-GO/BPPO membrane. It suggests that more water passageways are formed in the PEI (1,800)-GO/BPPO membrane. This is also the reason

why the rejection of PEI (1,800)-GO/BPPO membrane is increased instead of drop in the case of its water permeability much higher compared with that of PEI (10,000)-GO/BPPO membrane. Therefore, a proper Mw of PEI can modify GO

effectively, which improves the dispersion, compatibility and interaction of inorganic particles in/with BPPO polymer matrix. As a result, a membrane with high hydrophilicity, less defects and more uniform structure is formed.

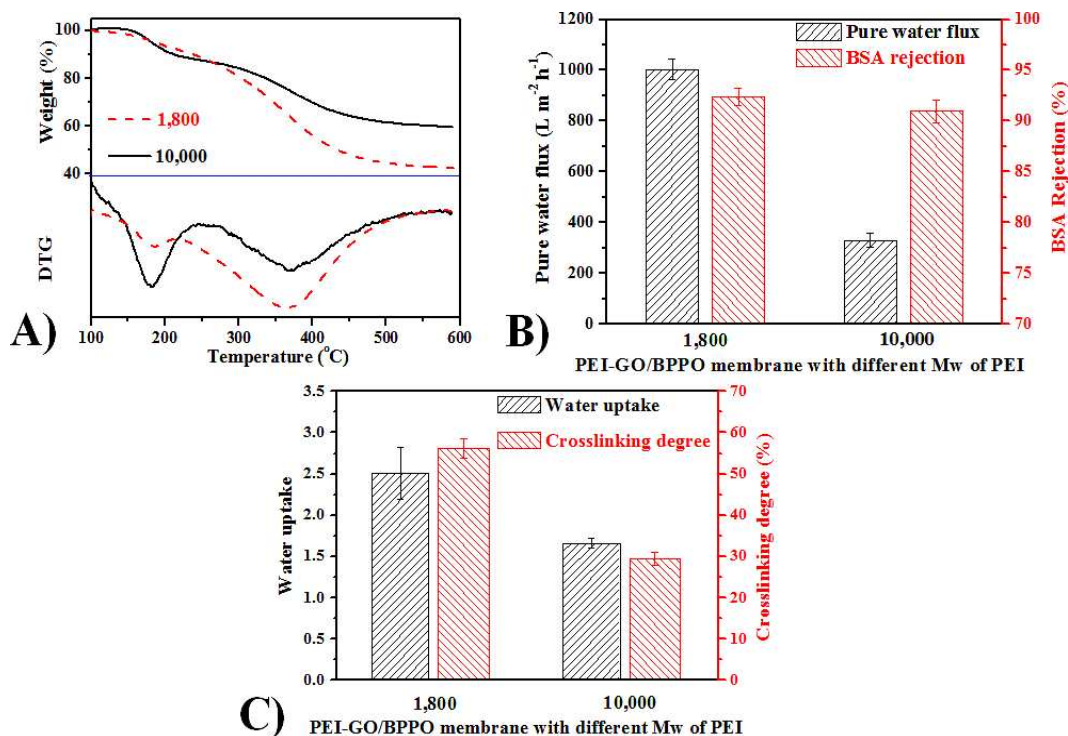


Fig. 5 (A) TGA/DTG measurement of PEI (10,000)-GO, dash line is the TGA/DTG measurement of PEI (1,800)-GO, (B) pure water fluxes and rejection tests to BSA (pH=4.7) and (C) water uptake and crosslinking degree of the PEI-GO/BPPO membrane with different molecular weight PEI. The contents of PEI-GO in the two composite membranes are 0.6% (w/w).

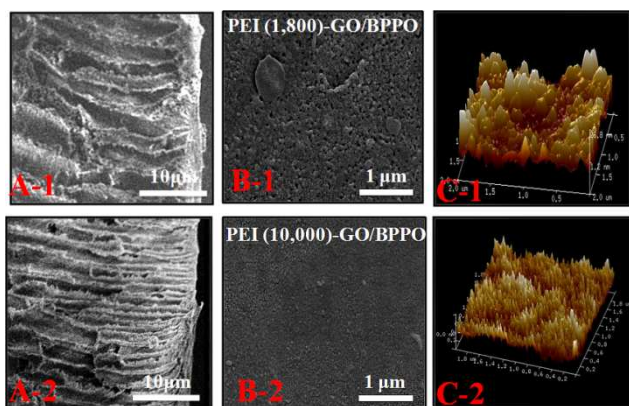


Fig. 6 (A) Cross-sectional SEM views, (B) surface views and (C) surface AFM three-dimensional surface of the PEI-GO/BPPO membrane with different molecular weight PEI ("1" and "2" represent the Mw of 1,800 and 10,000 respectively). The contents of PEI-GO in the two composite membranes are 0.6% (w/w).

### 3.4 Effect of weight fraction of PEI-GO on the membrane performance and morphologies

To gain a comprehensive insight into the influence of PEI (1,800)-GO content on the membrane performance, the membranes containing PEI-GO content ranged from 0.2% to 1.0% (w/w) with respect to BPPO content were prepared. The BPPO membrane without PEI-GO was also prepared for comparison.

Fig. 7B shows the crosslinking degrees of membranes with different weight fractions of PEI-GO. Obviously, the crosslinking degree of the PEI-GO/BPPO membrane is higher than that of the pristine BPPO membrane and increases as PEI-GO content enhances. It suggests that the covalently bonding interactions between PEI-GO and BPPO matrix leads to a network in which PEI-GO serves as the joints and crosslinkages. The water flux and rejection of membranes with different PEI-GO contents are shown in Fig. 7A. With the content of PEI-GO increasing, the water flux significantly enhances until a maximum (1064 L·m<sup>-2</sup>·h<sup>-1</sup>) at PEI-GO content of 0.6% (w/w), almost 6 times higher than that of the pristine BPPO membrane. However, the permeation rate of composite membrane decreases if continually adding PEI-GO. The rejection to BSA test has a contrary trend, which is consistent with the "trade-off" effect. The promotion of water permeation is attributed to the hydrophilicity of PEI-GO. In a detailed way, two factors, membrane hydrophilicity, porous and surface structure, are concerned.

The first factor is the high hydrophilicity of the composite membrane. Fig. 7C shows the WU capability of membranes with different weight fractions of PEI-GO. The PEI-GO/BPPO composite membrane exhibits higher WU than that of the pristine BPPO membrane. This is attributed to the hydrophilic group of PEI-GO, which effectively interacts with water molecules and forms water passageways, thereby enhancing the permeation. The decrease in WU of membrane at high PEI-GO content is probably due to the aggregation of particles. The second factor is the

structural differences of the composite membrane. As discussed above, the hydrophilic PEI-GO accelerates the exchange rate between solvent and non-solvent during phase inversion, which correspondingly forms membrane with more porous structure and rougher surface. In Fig. 8A, a slight expansion of finger-like structure in the composite membranes is observed, especially in the PEI-GO/BPPO-0.6 composite membrane. Besides, from Fig. 8 (B and C) and Table 3, the order of increasing roughness with

loading of PEI-GO, employing Rq, is:  $0\% < 0.2\% < 1.0\% < 0.4\%$   
 $10 < 0.8\% < 0.6\%$  (w/w). When the loading is beyond 0.6% (w/w), the PEI-GO may aggregate and the viscosity of the casting solution increases, thus suppressing the exchange between solvent and non-solvent<sup>20,34</sup>. The composite membrane turns out to be smoother surface and less porous and lower porosity structure, which leads to a decrease in water flux.

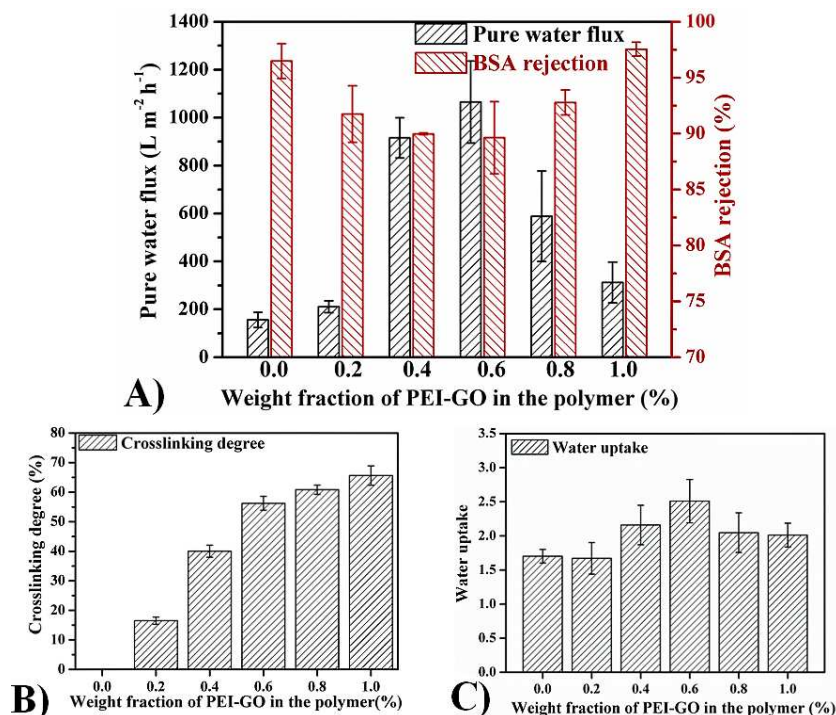


Fig. 7 (A) Pure water flux and rejection tests to BSA (pH=4.7) at 0.2 MPa, (B) crosslinking degree and (C) water uptake of membranes with different weight fractions of PEI-GO in BPPO polymer.

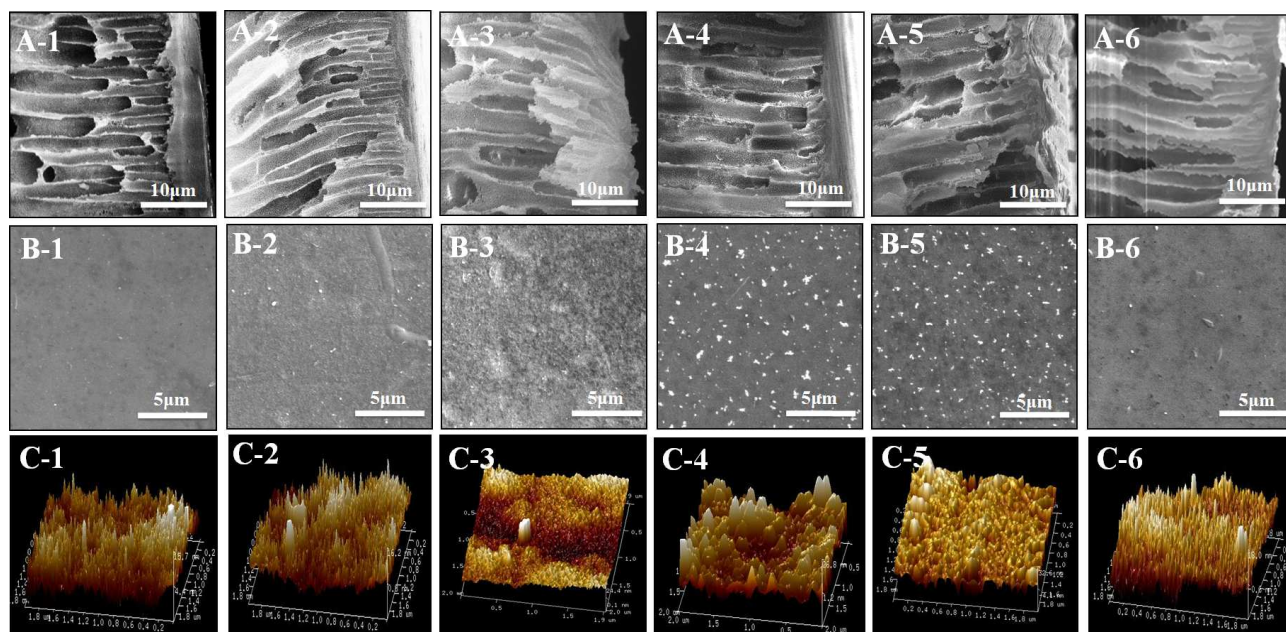


Fig. 8 (A) The cross-sectional SEM views, (B) surface SEM pictures and (C) surface AFM three-dimensional surface of membranes with different weight fractions of PEI-GO in BPPO polymer.

"1-6" refers to membrane with 0, 0.2, 0.4, 0.6, 0.8 and 1.0% (w/w) loading of PEI-GO in BPPO polymer respectively.

**Table 3** Surface roughness values of different weight fractions of PEI-GO in BPPO by AFM.

Weight fraction of PEI-GO in BPPO (%)	Rq (nm)	Ra (nm)
0	2.9	2.3
0.2	4.1	3.2
0.4	8.1	5.4
0.6	9.3	7.4
0.8	8.6	6.2
1.0	5.4	4.3

### 3.5 Anti-fouling performance of membranes

As is well known, the increase in surface roughness always decreases the anti-fouling property of membrane due to the contamination tends to accumulate in the "valleys" of rough membrane surface<sup>53</sup>. In this study, the PEI-GO/BPPO membrane has highly improved flux partly attributed to the increase in

surface roughness. We wonder whether the anti-fouling property of PEI-GO/BPPO membrane may drop. Fig. 9 shows the results of anti-fouling performances of BPPO, GO/BPPO, and PEI-GO/BPPO membrane, respectively. Interestingly, the flux recovery ratio of PEI-GO/BPPO membrane doesn't decrease but increase. Besides, the reversible resistance of PEI-GO/BPPO membrane is 50%, which is much higher than that of BPPO membrane (28%). We speculate that it is attributed to the high hydrophilicity of PEI-GO/BPPO membrane as it forms hydrated layers to inhibit protein adsorption. Moreover, the electrostatic repulse interaction between BSA molecule and the PEI-GO/BPPO membrane at pH=4 is stronger, thus better enhancing protein adsorption resistance. Combining the stability test that PEI-GO/BPPO shows a stable and good flux recovery, the results suggest that the BPPO membrane incorporated with PEI-GO has a fairly favourable anti-fouling performance and huge potential in practical applications.

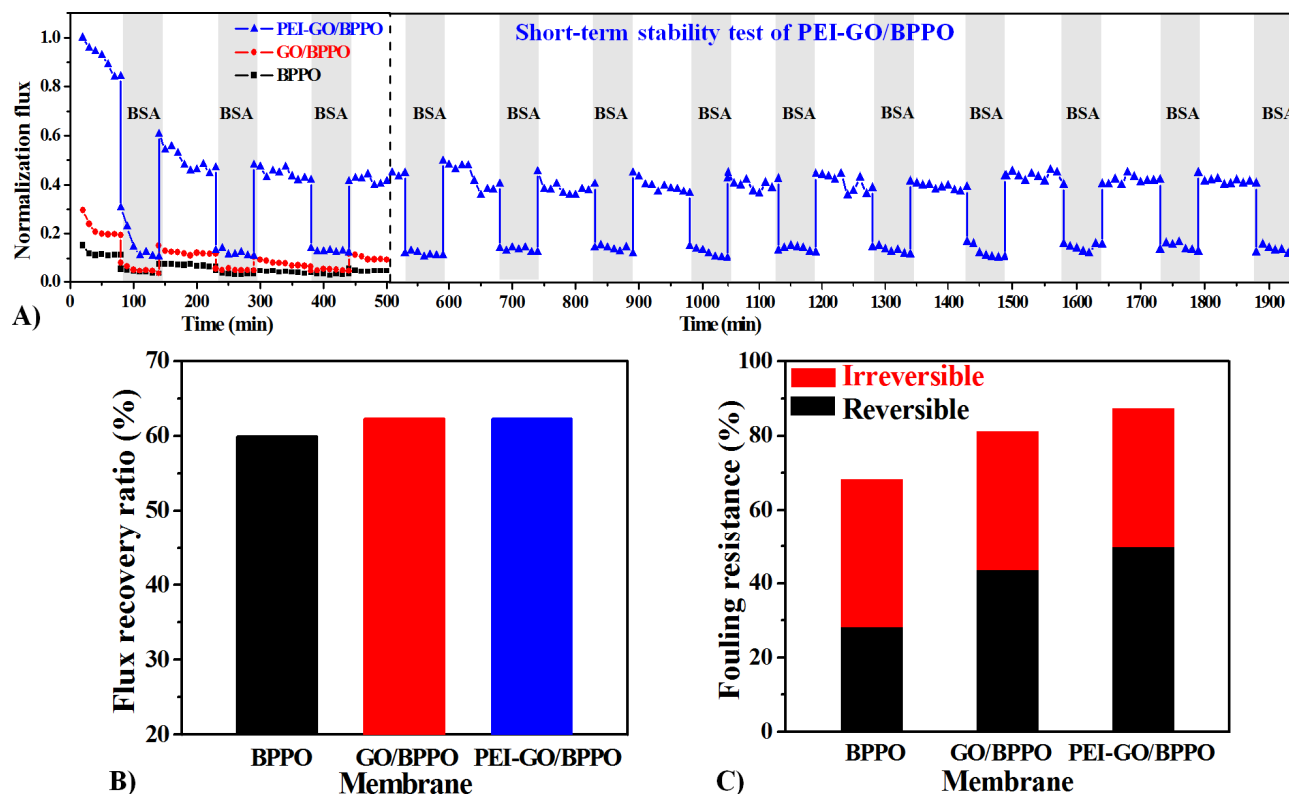


**Fig. 9** (A) Time-dependent fluxes of membranes with different components during BSA filtration, and a short-term stability performance of PEI-GO/BPPO composite membrane, (B) flux recovery ratio of tested membranes and (C) fouling resistance of tested membranes.

## 4 Conclusions

In this work, PEI-GO has been synthesized by modified "one-spot" method and incorporated into BPPO to prepare a novel UF membrane via phase inversion method. The covalently bonding interactions between PEI-GO and benzyl bromide of BPPO facilitate PEI-GO's dispersion and compatibility with BPPO, which endows the PEI-GO/BPPO membrane with a uniform, less defects and hydrophilic cross-linking network structure. Besides, the amine groups of PEI-GO make the membrane more hydrophilic, which leads to rougher membrane surface and more

porous structure due to the quicker phase inversion. Therefore, a composite membrane exhibiting highly improved water flux simultaneously maintaining high rejection is obtained. The work also has been investigated the effects of PEI's molecular weight and PEI (1,800)-GO's weight fraction on membrane performance. It has been found that PEI with proper Mw and an appropriate PEI-GO loading are a premise to prepare high performance membrane. Additionally, BPPO membrane incorporated with PEI-GO has a fairly favourable anti-fouling and stable performance. Therefore, the PEI-GO/BPPO membrane presents a huge potential in practical water treatment.

## Nomenclature

F	water flux
V	total volume of permeated pure water
A	membrane area
t	operation time
R	rejection
C <sub>p</sub>	concentration of the permeation solution
C <sub>f</sub>	concentration of the feed solution
D	crosslinking degree
W <sub>2</sub>	weight of the treated membrane sample
W <sub>1</sub>	weight of the original membrane sample
FRR	flux recovery ratio
J <sub>R</sub>	pure water flux of cleaned membrane
J <sub>0</sub>	pure water flux of original membrane
J <sub>p</sub>	flux of protein solution
R <sub>r</sub>	reversible fouling resistance
R <sub>ir</sub>	irreversible fouling resistance

## Acknowledgements

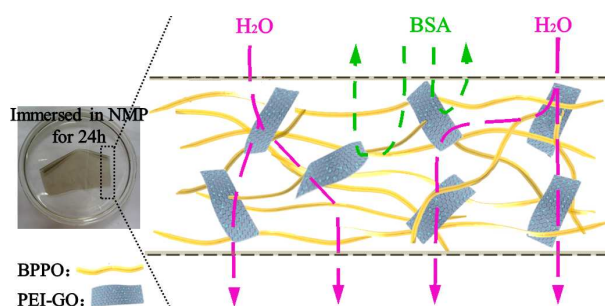
This work was supported by the National Natural Science Foundation of China (NSFC) (No. 21276051), Chinese doctoral fund (20110071130001), the Natural Science Foundation of Shanghai (No. 12ZR1401900), and the National Basic Research Program of China (2009CB930000).

## Notes and references

- 10 *State Key Laboratory of Molecular Engineering of Polymers, Department of Macromolecular Science, Laboratory of Advanced Materials, Fudan University, Shanghai, 200433, P. R. China.*  
*E-mail: bbtang@fudan.edu.cn, or peiyiwu@fudan.edu.cn.*
- M. A. Shannon, P. W. Bohn, M. Elimelech, J. G. Georgiadis, B. J. Marinas and A. M. Mayes, *Nature*, 2008, **452**, 301-310.
  - H. Y. Ma, C. Burger, B. S. Hsiao and B. Chu, *ACS Macro Lett.*, 2012, **1**, 723-726.
  - F. Qu, H. Liang, Z. Wang, H. Wang, H. Yu and G. Li, *Water Res.*, 2012, **46**, 1490-1500.
  - F. S. Qu, H. Liang, J. Zhou, J. Nan, S. L. Shao, J. Q. Zhang and G. B. Li, *J. Membr. Sci.*, 2014, **449**, 58-66.
  - W. Gao, H. Liang, J. Ma, M. Han, Z. L. Chen, Z. S. Han and G. B. Li, *Desalination*, 2011, **272**, 1-8.
  - F. Zhang, W. B. Zhang, Y. Yu, B. Deng, J. Y. Li and J. Jin, *J. Membr. Sci.*, 2013, **432**, 25-32.
  - Z. H. Wang, H. R. Yu, J. F. Xia, F. F. Zhang, F. Li, Y. Z. Xia and Y. H. Li, *Desalination*, 2012, **299**, 50-54.
  - J. G. Zhang, Z. W. Xu, M. J. Shan, B. M. Zhou, Y. L. Li, B. D. Li, J. R. Niu and X. M. Qian, *J. Membr. Sci.*, 2013, **448**, 81-92.
  - S. J. Lee, M. Dilaver, P. K. Park and J. H. Kim, *J. Membr. Sci.*, 2013, **432**, 97-105.
  - H. Wu, B. B. Tang and P. Y. Wu, *J. Phys. Chem. C*, 2012, **116**, 2246-2252.
  - M. Hebrant, M. Rose-Helene and A. Walcarius, *Colloid Surf. A-Physicochem. Eng. Asp.*, 2013, **417**, 65-72.
  - L. J. Zhu, L. P. Zhu, J. H. Jiang, Z. Yi, Y. F. Zhao, B. K. Zhu and Y. Y. Xu, *J. Membr. Sci.*, 2014, **451**, 157-168.
  - J. Huang, K. S. Zhang, K. Wang, Z. L. Xie, B. Ladewig and H. T. Wang, *J. Membr. Sci.*, 2012, **423**, 362-370.
  - Q. Wang, X. Wang, Z. Wang, J. Huang and Y. Wang, *J. Membr. Sci.*, 2013, **442**, 57-64.
  - N. Maximous, G. Nakhla, W. Wan and K. Wong, *J. Membr. Sci.*, 2010, **352**, 222-230.
  - M. Fang, K. G. Wang, H. B. Lu, Y. L. Yang and S. Nutt, *J. Mater. Chem.*, 2009, **19**, 7098-7105.
  - S. Stankovich, D. A. Dikin, R. D. Piner, K. A. Kohlhaas, A. Kleinhammes, Y. Jia, Y. Wu, S. T. Nguyen and R. S. Ruoff, *Carbon*, 2007, **45**, 1558-1565.
  - F. M. Jin, W. Lv, C. Zhang, Z. J. Li, R. X. Su, W. Qi, Q. H. Yang and Z. M. He, *RSC Adv.*, 2013, **3**, 21394-21397.
  - S. Zinadini, A. A. Zinatizadeh, M. Rahimi, V. Vatanpour and H. Zangeneh, *J. Membr. Sci.*, 2014, **453**, 292-301.
  - J. Lee, H. R. Chae, Y. J. Won, K. Lee, C. H. Lee, H. H. Lee, I.-C. Kim and J.-m. Lee, *J. Membr. Sci.*, 2013, **448**, 223-230.
  - C. Zhao, X. Xu, J. Chen and F. Yang, *J. Environ. Chem. Eng.*, 2013, **1**, 349-354.
  - Y. F. Zhao, Z. W. Xu, M. J. Shan, C. Y. Min, B. M. Zhou, Y. L. Li, B. D. Li, L. S. Liu and X. M. Qian, *Sep. Purif. Technol.*, 2013, **103**, 78-83.
  - S. S. Madaeni, S. Zinadini and V. Vatanpour, *J. Membr. Sci.*, 2011, **380**, 155-162.
  - M. S. Mauter, Y. Wang, K. C. Okemgbo, C. O. Osuji, E. P. Giannelis and M. Elimelech, *ACS Appl. Mater. Interfaces*, 2011, **3**, 2861-2868.
  - J. D. Schiffman, Y. Wang, E. P. Giannelis and M. Elimelech, *Langmuir*, 2011, **27**, 13159-13164.
  - H. J. Song and C. K. Kim, *J. Membr. Sci.*, 2013, **444**, 318-326.
  - H. J. Song, Y. J. Jo, S. Y. Kim, J. Lee and C. K. Kim, *J. Membr. Sci.*, 2014, **466**, 173-182.
  - L. Yu, Y. T. Zhang, B. Zhang, J. D. Liu, H. Q. Zhang and C. H. Song, *J. Membr. Sci.*, 2013, **447**, 452-462.
  - L. Gao, B. B. Tang and P. Y. Wu, *J. Membr. Sci.*, 2009, **326**, 168-177.
  - B. B. Tang, T. W. Xu and W. H. Yang, *J. Membr. Sci.*, 2006, **268**, 123-131.
  - K. Feng, Y. W. Cao and P. Y. Wu, *J. Mater. Chem.*, 2012, **22**, 11455-11457.
  - K. Feng, B. Tang and P. Wu, *ACS Appl. Mater. Interfaces*, 2013, **5**, 1481-1488.
  - H. Y. Liu, T. Kuila, N. H. Kim, B. C. Ku and J. H. Lee, *J. Mater. Chem. A*, 2013, **1**, 3739-3746.
  - H. Wu, B. Tang and P. Wu, *J. Membr. Sci.*, 2010, **362**, 374-383.
  - B. B. Tang, T. W. Xu, P. J. Sun and W. H. Yang, *J. Membr. Sci.*, 2006, **279**, 192-199.
  - L. Yang, B. Tang and P. Wu, *J. Membr. Sci.*, 2014, **467**, 236-243.
  - H. Wu, B. Tang and P. Wu, *J. Membr. Sci.*, 2014, **451**, 94-102.
  - Y. Li, T. W. Xu and M. Gong, *J. Membr. Sci.*, 2006, **279**, 200-208.
  - X. H. Zhou, Z. X. Chen, D. H. Yan and H. B. Lu, *J. Mater. Chem.*, 2012, **22**, 13506-13516.
  - L. M. Zhang, Z. X. Lu, Q. H. Zhao, J. Huang, H. Shen, and Z. J. Zhang, *small*, 2011, **7**, 460-464.
  - O. C. Compton, D. A. Dikin, K. W. Putz, L. C. Brinson and S. T. Nguyen, *Adv. Mater.*, 2010, **22**, 892-896.
  - Y. X. Xu, H. Bai, G. W. Lu, C. Li and G. Q. Shi, *J. Am. Chem. Soc.*, 2008, **130**, 5856-5857.
  - P. Song, X. Y. Zhang, M. X. Sun, X. L. Cui and Y. H. Lin, *RSC Adv.*, 2012, **2**, 1168-1173.
  - X. Cai, M. S. Lin, S. Z. Tan, W. J. Mai, Y. M. Zhang, Z. W. Liang, Z. D. Lin and X. J. Zhang, *Carbon*, 2012, **50**, 3407-3415.
  - L. Z. Feng, S. A. Zhang and Z. A. Liu, *Nanoscale*, 2011, **3**, 1252-1257.
  - R. R. Nair, H. A. Wu, P. N. Jayaram, I. V. Grigorieva and A. K. Geim, *Science*, 2012, **335**, 442-444.
  - B. Tang, T. W. Xu, M. Gong and W. H. Yang, *J. Membr. Sci.*, 2005, **248**, 119-125.
  - L. Yan, Y. S. Li, C. B. Xiang and S. Xianda, *J. Membr. Sci.*, 2006, **276**, 162-167.
  - J. G. Zhang, Z. W. Xu, W. Mai, C. Y. Min, B. M. Zhou, M. J. Shan, Y. L. Li, C. Y. Yang, Z. Wang and X. M. Qian, *J. Mater. Chem. A*, 2013, **1**, 3101-3111.
  - X. Bai, Y. T. Zhang, H. Wang, H. Q. Zhang and J. D. Liu, *Desalination*, 2013, **313**, 57-65.
  - C. Madigan, Y. K. Leong and B. C. Ong, *Int. J. Miner. Process.*, 2009, **93**, 41-47.
  - H. Kim, R. Namgung, K. Singha, I.-K. Oh and W. J. Kim, *Bioconjugate Chem.*, 2011, **22**, 2558-2567.

53 Z. Xu, J. Zhang, M. Shan, Y. Li, B. Li, J. Niu, B. Zhou and X. Qian, *J. Membr. Sci.*, 2014, **458**, 1-13.

For TOC only



PEI-GO/BPPO membrane with rougher surface and hydrophilic cross-linking network is formed by PEI-GO covalently bonded with BPPO.